

Project Report on

“PHOTOGRAMMETRY FOR NON-CONTACT MEASUREMENT OF DEFLECTION”



Submitted by:

ASHIMA SETIA

2006CE10254

Under the Guidance of:

DR. S. BHALLA

In partial fulfillment of the requirements of the degree of

Bachelor of Technology

to the

Department of Civil Engineering,

Indian Institute of Technology Delhi

April 2010

CERTIFICATE

I do certify that this report explains the work carried out by me in the courses CED411 (Project-Part 1) and CED412 (Project–Part 2), under the overall supervision of Dr. Suresh Bhalla. The contents of the report including text, figures, tables, computer programs, etc. have not been reproduced from other sources such as books, journals, reports, manuals, websites, etc. Wherever limited reproduction from another source had been made the source has been duly acknowledged at that point and also listed in the References.

Ashima Setia

April 26, 2010

CERTIFICATE

“This is to certify that the report submitted by Ms. Ashima Setia describes the work carried out by her in the courses CED411 (Project- Part 1) and (CED412 Project–Part 2), under my overall supervision.”

Dr. Suresh Bhalla

(Supervisor)

Date: April

ACKNOWLEDGEMENT

I would like to express my sincere thanks & gratitude to Dr. Suresh Bhalla for his continuous and unrelenting support, guidance and help, which have been invaluable during the course of this project. His knowledge, insight and constant motivation at each step of the project has been instrumental in its completion.

I would like to express my thanks to Dr. Vasant Matsagar for his support and contribution.

I would also like to thank Mr. Nitin Chaurasiya, Mr. Lal Singh, Mr. Bir Singh and Mr. Gautam for their invaluable support during lab work.

ABSTRACT

Photogrammetry is the art science and technology of taking measurements with the help of photographs. The technique is based on the geometry of perspective scenes and on the principles of stereovision, and actually pre-dates the invention of photography. The ever-expanding areas of application of close-range photogrammetry can be grouped into three major areas: architectural photogrammetry, biomedical and bioengineering photogrammetry (biostereometrics) and industrial photogrammetry. The technique is becoming popular because of its low cost, ability to conduct measurements in inaccessible areas and reasonable level of precision. The present study aims at using photogrammetry technique to carry out measurements in virtual labs. Virtual labs enable the students to conduct experiments involving measurement of distances without being physically present in the lab. The project aims at using photogrammetry technique to measure deflection of structures. Images are processed using MATLAB image processing functions, which are written in the form of a code. The program is run on some lab experiments. The deflection values obtained from the pictures are compared with the actual values. A reasonable precision is reached. The sources of error, limitations and precautions to avoid wrong results are identified. Thus, a cost-effective, reasonably accurate and convenient method for measurement of structural deflections is achieved.

CHAPTER 1

INTRODUCTION

1.1 NEED FOR PHOTOGRAMMETRY

A major difficulty in the testing and evaluation of bridges in the field is the measurement of vertical deflection. The use of instruments such as mechanical dial gauges, linear potentiometers, linear variable differential transducers (LVDTs) and other similar types of deflection transducers is usually not feasible, because a fixed base is needed from which relative displacements are measured. This often requires access under the structure to erect a temporary support to mount the instrument or for running a wire from the instrument to the ground. These difficulties can be eliminated using photogrammetry, which is a noncontact deflection measurement technique. Photogrammetry offers the capability to measure the spatial coordinates of discrete points on a bridge in three dimensions without having to touch the structure. Other systems are available that provide noncontact measurement capabilities using laser technology, however, at a higher cost. A photogrammetric system operates at a fraction of the cost of laser-based systems and is thus more likely to fit within the budget of most projects. (Jauregui, 2003)

1.2 PHOTOGRAMMETRY: DEFINITION

Photogrammetric surveying is a method where three-dimensional measurements are made from two-dimensional photographs taken of an object. In general, photographs are taken of an object from at least two camera positions. From each camera position, there is a line of sight that runs from each point on the object to the perspective center of the camera. Using the principle of triangulation, the point of intersection between the different lines of sight for a particular point is determined mathematically to identify the spatial or three-dimensional location of the object point. Photogrammetry may be classified as either aerial or terrestrial. In aerial photogrammetry, photographs are taken of an area from an airplane flying overhead, while in terrestrial photogrammetry, the photographs are taken from stations situated close to or on the earth's surface (Hilton 1985). When pictures are taken of an object within the range of 100 mm (4 in.) to

100 m (330 ft), photogrammetry is further defined as close-range terrestrial photogrammetry (Hilton 1985).

1.3 STEPS IN PHOTOGRAMMETRY

There are four basic steps in the photogrammetric process:

1. Layout of the control or reference coordinate system
2. Planning and taking the photographs
3. Processing the photography
4. Point measurement using the photographs (Hilton 1985)

A network of control points, i.e., locations with known X, Y, and Z coordinates and/or calibrated distance bars is used to establish scale between the photographs and the real structure.

1.4 CAMERA

The camera types commonly used in photogrammetry are metric and semimetric, both of which are configured for photogrammetric surveying purposes and are thus provided with reference or fiducial marks in order to establish the internal camera properties. Metric cameras, like the Zeiss camera series, are high precision cameras often used for aerial surveys and are generally more expensive than semimetric cameras. To be used for photogrammetric work, the camera must first be calibrated to determine its internal attributes such as lens distortion and focal length. Steps involved in the calibration process are discussed in detail in the *FotoG-FMS User Manual, 2000*.

Processing and measurement of the photographs consists of four phases :

1. relative orientation,
2. Block formation
3. Absolute orientation
4. Bundle adjustment (*FotoG-FMS User Manual, 2000*).

Better photogrammetric accuracy is achieved under the following conditions (Jauregui et al.):

1. Better distribution of control points
2. The use of double-sided targets
3. Closer camera-to-object distance
4. Better lighting

1.5 Image Theory

An image is a 2-dimensional light intensity function $f(x, y)$ where x and y denote spatial coordinates and the value of f at any point is proportional to the brightness or gray level. Image that has been discretized both in spatial coordinates and brightness is called a digital image. The elements of this digital array are called pixels.

1.6 IMAGE PROCESSING AND PRECISION

Processing and measurement of the photographs consists of four phases

1. relative orientation
2. block formation
3. absolute orientation
4. bundle adjustment (*FotoG-FMS User Manual ~2000*).

In general, use of a high-resolution camera and automatic point correspondence gives high levels of accuracy. Following excerpts give the level of accuracy achieved in various experiments conducted in the past:

1. Nastasia (1998) reported on an automated DCRTP system for highway design and maintenance. The system was developed under a small business innovative research (SBIR) grant from the National Science Foundation to provide an automated, portable way of modelling highway roadside features such as rock faces, slopes, bridges, riverbanks, tunnels, and culverts, which can be difficult to measure using aerial photography methods. Equipment included a high resolution digital camera (similar to the one used in this study mounted on a total station).

During the image processing, points were automatically identified and referenced between the images to provide three-dimensional coordinates at an accuracy of 6 cm (2.36 in.). The use of automatic instead of manual point correspondence is shown to greatly improve the efficiency of the photogrammetric system; however, the accuracy must be improved before it may be used for bridges where deformations are small.

2. In Forno et al. (1991), deflection measurements of an arch bridge tested to failure were made with moiré photography and photogrammetry. For the photogrammetric study, results showed that an accuracy of 0.2 mm (0.008 in.) was possible using a high-quality Zeiss metric camera.
3. Johnson (2001) used a photogrammetric system to measure the geometry of the Waldo–Hancock Bridge in the state of Maine. The suspension bridge was built in 1931 and is 622 m (2,040 ft) long. Due to severe deterioration of the superstructure and the deck, the Maine Department of Transportation chose to rehabilitate this heavily travelled bridge. To aid in the rehabilitation, the geometry of the bridge was needed. Circular targets were mounted at numerous locations on the bridge and a global positioning system (GPS) was used for control purposes. Digital photographs were taken with a Kodak DCS series camera from a low-flying helicopter in order to minimize traffic disruption. The photogrammetry activities (not including target installation and GPS control measurements) took approximately 10 h of field time and one person processed the images over a three-week period. The reported quality of the measurements included a relative accuracy of 15.9 mm (0.625 in.) over a range of 640 m (2,100 ft) and a local accuracy of 3.2 mm (0.125 in.) over 210 m (700 ft).

As a summary of the application of close-range photogrammetry in the field of structural engineering, Mills and Barber, 2004 reviewed the state-of-the-art of the technique in this field and observed the following:

- Improved photogrammetry network design such as multi-station convergent networks provides better accuracy, precision, and reliability;

- Camera self-calibration and analytical processing techniques allow the use of non-metric cameras and a simplified camera calibration process;
- More low cost software packages are available to users;
- Development of internet technology has made on-line photogrammetric measurements possible;
- Advances in digital techniques have eliminated the inconvenient image digitalization process, and have provided users a complete digital workflow; and
- Modern digital cameras and better analytical tools provide more flexibility and improved efficiency for photogrammetric measurements.

CHAPTER 2

HISTORY

The history of close-range photogrammetry can be traced back to the late 1840s when the first photogrammetry system was developed by Aimé Laussedat, a colonel in the French Army Corps of Engineers. In 1849, Laussedat first utilized terrestrial photographs to compile maps, and the approach was officially accepted by the Science Academy in Madrid in 1862. Laussedat later made a plan of Paris from photographs taken from building rooftops, which was exhibited at the Paris Exposition in 1867. Another pioneer in the field of close-range photogrammetry is the Prussian architect, Meydenbauer. He recorded many historical monuments, churches, and buildings with a close-range photogrammetry method based on Laussedat's techniques. In 1885, Meydenbauer established a state institute in Berlin to record architectural buildings.

The pioneering accomplishments of Laussedat, Meydenbauer, and many other photogrammetrists led to the formation of the International Society for Photogrammetry (ISP) in 1910, one of the most important events in the history of photogrammetry. The technical commissions of the society began work in specific areas of photogrammetry in 1926, including aerial, terrestrial, architectural, and engineering photogrammetry. Since then, close-range photogrammetry was considered a branch of terrestrial photogrammetry and was virtually ignored until the 1960s when photogrammetrists began to use inexpensive, non-customized (off-the-shelf) cameras for image collection. By the 1970s, the use of close-range photogrammetry accelerated due to the rapid development in computer technology and expanded at even a faster rate in the 1990s as the digital era emerged. (Adams, L.P., 1975.)

CHAPTER 3

LITERATURE REVIEW

Research activity on the application of close-range photogrammetry in bridge-related projects has been minimal and widely dispersed within the last 25 years.

1. Photogrammetry was used by Scott (1978) to measure local buckling deformations in a curved, steel box-girder bridge. The continuous bridge was a 1:12 scale model tested to failure over 11 days. About 4,000 targets were attached to the compression flange steel plate close to an interior support; however, only 1,800 were used for measurement purposes. An accuracy of 0.2 mm (0.008 in.) was achieved using a stereo-metric camera, but at high cost as compared with dial indicators. Theodolite observations took two people four days each while data analysis took 44 days.

2. Bales (1985) reported on the use of close-range photogrammetry for various bridge applications. In the first application, a condition survey was done using photogrammetry to find delaminations and estimate the size of cracks in a reinforced concrete bridge deck. In the second application, the deflection of a rail bridge caused by thermal effects was measured photogrammetrically. In the third application, the writer examined the effect of dead load caused by the weight of the concrete deck on the girders of a three-span continuous steel bridge under construction. The average difference in deflection between photogrammetry and a conventional level was 3 mm (0.12 in.). The maximum difference was 9 mm (0.36 in.). The writer concluded that accuracies in the order of 3.2 mm (0.125 in.) can be achieved in measuring bridge deflections using a Zeiss metric camera.

3. Johnson (2001) used a photogrammetric system to measure the geometry of the Waldo–Hancock Bridge in the state of Maine. The suspension bridge was built in 1931 and is 622 m (2,040 ft) long. Due to severe deterioration of the superstructure and the deck, the Maine Department of Transportation chose to rehabilitate this heavily traveled bridge. To aid in the rehabilitation, the geometry of the bridge was needed. Circular

targets were mounted at numerous locations on the bridge and a global positioning system (GPS) was used for control purposes. Digital photographs were taken with a Kodak DCS series camera from a low-flying helicopter in order to minimize traffic disruption. The photogrammetry activities (not including target installation and GPS control measurements) took approximately 10 h of field time and one person processed the images over a three-week period. The reported quality of the measurements included a relative accuracy of 15.9 mm (0.625 in.) over a range of 640 m (2,100 ft) and a local accuracy of 3.2 mm (0.125 in.) over 210 m (700 ft).

4. Abdel-Sayed et al. reported the use of close-range photogrammetry for the deformation monitoring of soil-steel bridges. The main objectives of the monitoring program were to determine the cross-sectional shape of the metal conduit at certain locations and to assess the deformations through periodic monitoring. Targets were 6 mm (0.25 in.) diameter retro-reflective circles, which were evenly distributed along the cross section. Scale rods were used consisting of retro-reflective targets on aluminum angles, which were placed in different directions in the object space to provide uniform object scale in all directions. Photographs were taken using a 24 mm (0.94 in.) wide-angle lens camera along the conduit at two locations for each section. The accuracy was evaluated by comparing the distances between points calculated by photogrammetry and obtained by direct measurements. For a structure having a span of approximately 4 m (12 ft), the mean difference of distances ranged from 2 to 7 mm (0.080 to 0.276 in.) for cross-sections having the scaling devices, and from 30 to 80 mm (1.18–3.15 in.) for cross-sections without the scaling devices. The mean difference of distances in the longitudinal direction ranged from 20 to 40 mm (0.787–1.575 in.).

5. The City University of London monitored the deformation of a military steel bridge. The measurements focused on an 18 m (59 ft) bridge section using seven camera stations, as shown in. A total of 768 measurements of target coordinates were made, the maximum standard deviations of which were found to be ± 0.39 mm (0.015 in.), ± 0.62 mm (0.024 in.), and ± 0.23 mm (0.009 in.) in the x , y , and z direction, respectively.

6. Forno et al. reported the studies performed at the University of Dundee in Scotland on the deformation measurement of a decommissioned masonry arch bridge and a full-scale laboratory model of the bridge. The bridge had a single closed-spandrel arch

with a 4 m (13.2 ft) diameter and overall dimensions of 6 m × 4 m × 6 m (20 ft × 13 ft × 20 ft, length × height × width). The bridge was tested under a concentrated load applied at the top of the spandrel. Both Moiré photography and close-range photogrammetry were applied to measure the deformation of the bridge. Moiré photography results provided control for the photogrammetric measurements since scale bars appeared too dark in the photos to serve as an accurate reference. The standard deviation of the photogrammetric measurement was approximately 0.2 mm or 0.008 in.

7. Woodhouse et al. conducted several high strength, concrete column tests. The aim of the tests was to determine the influence of steel hoop reinforcement on the failure of the columns. Column deflection was monitored during the tests by close-range photogrammetry. Linear variable displacement transducers (LVDT) were used to measure deformation of the column for comparison. Four digital cameras were used, two of which had a resolution of 1534 × 1024 pixels and the other two, 1008 × 1018 pixels. A vision metrology system was used which was controlled remotely in such a way that images were captured automatically and synchronously by the four cameras.

8. Fraser and Riedel performed a study on the monitoring of thermal deformations of steel beams. The temperature variation of the steel beams ranged from 1100 °C down to 50 °C, and the measurement rate was one set every 15 s. In order to collect approximately 70–80 sets of measurements in about 2 h, a highly automated, on-line data processing system was used. Two groups of targets were utilized. Group 1 had about 10 to 15 targets, and was used to monitor the deformation of the beam; group 2 had about 30 targets that were placed on the wall behind the beams and stayed stationary during the entire test, serving as reference points. The average camera-to-object distance for the outer cameras was 9.6 m (31.7 ft), and 6.7 m (22.1 ft) for the center camera. An Australis[®] system was used for the off-line photogrammetric analysis, which was modified for the on-line process of real time measurement. The coordinate changes of the targets on the steel beam were recorded continuously over time. The final RMS value of coordinate residuals in approximately 800 point measurements averaged 1.6 μm (close to 0.2 pixels), which yielded an accuracy in the object space of 0.7–1.3 mm (0.03–0.05 in.).

9. Jauregui et al. conducted a study of vertical deflection measurement of bridges using digital close-range terrestrial photogrammetry (DCRTP). The study consisted of a

laboratory and two field exercises. In the laboratory exercise, photogrammetric measurements of a 11.6 m (38 ft) steel beam loaded at midspan were made and compared with dial gauge readings and elastic beam theory. In the first field exercise, the initial camber and dead load deflection of 31.1 m (102 ft) prestressed concrete bridge girders were measured photogrammetrically and compared with level rod and total station readings. A comparison of the photogrammetric measurements with the dead load deflection diagram was also made. In the second field exercise, the vertical deflection of a 14.9 m (49 ft) noncomposite steel girder bridge loaded with two dump trucks was measured. Photogrammetric results were compared with deflections estimated using elastic finite-element analysis, level rod readings, and curvature-based deflection measurements. The paper presents suggestions to bring out improvement in DCRTTP technique.

Fig. 3. 1. Plan view of Las Alturas Bridge



CHAPTER 4

AIMS OF THE PROJECT

Virtual lab has been added as a new feature in Smart Structural Dynamics Laboratory. In order to eliminate the need to read the deflection values from dial gauge, an image is captured and processed to calculate deflection values. This technique is particularly useful in inaccessible areas. Image processing is done by manual method in part I. For automatic processing, an algorithm is made, keeping in mind properties of MATLAB image processing function. In part II, digital image processing has been done by using MATLAB image processing toolbox and the setup has been applied to ongoing lab experiments in order to determine its accuracy.

4.1 project outline: The project aims to accomplish the following:

1. Capturing images from the experiment before and after deflection using a digital camera
2. Manual image processing to remove unwanted features
3. Digital image processing using MATLAB to obtain coordinates
4. Calculation of deflection using scale obtained
5. Comparison of results with physical measurements (e.g., values from dial gauge readings)

4.2 Virtual Lab Apparatus

The aim of the project is to develop a mechanism to measure deflection of structures using techniques of non-contact measurement. The virtual lab provides the facility to capture the image of an apparatus in the lab. Part 1 of the project aims at measuring deflection of a beam using photogrammetric technique and image processing by MATLAB.

Apparatus:

1. Beam
Length= 0.56m, width= 0.019m, thickness= 0.0015m, E= 70 GPa
2. Load= 0.201kg point load

3. Camera: TV lens 6mm 1/3 inch; model :CS adon system, SONY vct r640 mi00620

Image is captured as an RGB image.

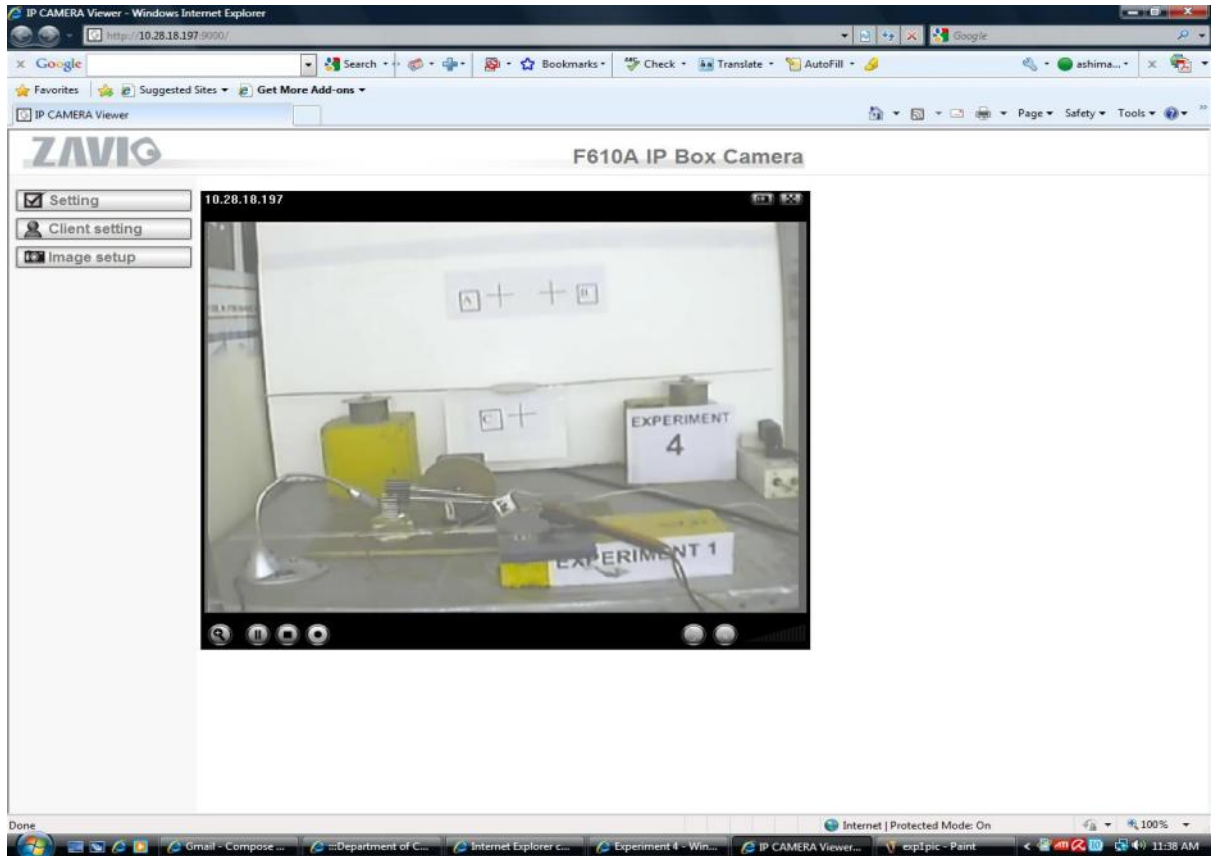


Fig. 5.1: snapshot of loaded beam

4.3 **Principle:** Two images of the experimental setup are captured, one at loaded and another at unloaded stage. The unloaded image gives the initial camber of the beam. A and B are reference points used as a scale. The distance AB is 100mm. Point C lies beneath the point load.

- a. The coordinates of the three points are determined in each image in the form of pixels.
- b. The scale of each image is obtained as: (actual distance between A & B/ pixel distance between A & B)
- c. Vertical distance between reference line and target is calculated. Change in this distance is the value of vertical deflection.

CHAPTER 5

APPROACHES FOLLOWED

Four different approaches were followed to attempt this task. The challenge was to locate the coordinates of required points by scanning the image. The required points were marked with special features and these features were fed in the program as the criteria for ‘picking’ the desired points. Four different approaches were followed.

5.1 Data Cursor using cross as reference and target points: partially successful

The image viewer provides a feature called data cursor that gives pixel coordinates of every point it is scrolled to. Ideally, the vertical and horizontal lines in a cross must intersect at a single point and pointing the data cursor to a cross gives its coordinates. The accuracy is low because the point of intersection of vertical and horizontal lines is not a single pixel in all cases. There may be human error also, since one may not point to the exact point just by looking in the image viewer. The values obtained for displacement are within acceptable range.

Using the data cursor, coordinates of the three points were obtained for the two images.

(in Pixels):

1. Table 5.1: Coordinates for Loaded state

Point	X	Y
A	524	348
B	579	344
C	547	493

2. Table 5.2:Coordinates for Unloaded state

Point	X	Y
A	525	348
B	580	344
C	547	491

Distance between A & B: 55.14 pixels

Actual length AB= 100mm

Deflection of point C= 2 pixels

Actual deflection= $(100/55.14) \times 2$ mm= 3.60 mm

Dial Gauge reading= 4.10 mm

5.2 Program to locate cross-shaped objects in an image: unsuccessful

The essence of the program is that MATLAB stores a grayscale image as a 2-dimensional array. The elements of the array give intensity of the points. Values for dark regions lie close to zero and for white regions, close to 255. The image is scanned as a grayscale image. Cross is the point for which movement in $\pm x$ $\pm y$ directions give a zero value. The output of the program gives coordinates of intersection of black lines, i.e., cross. The coordinates of the three crosses can be stored and processed to get the distance. Distance AB is used as a scale for conversion of pixels to mm. MATLAB is used for image processing. MATLAB stores images in the form of two-dimensional (grayscale) or three dimensional arrays (RGB). The camera captures an image in RGB format. A grayscale image assigns values ranging from zero to 255, with the value zero corresponding to the darkest points. Therefore, points with zero intensity (i.e. , value zero) can be detected. A cross corresponds to a point having value zero on moving in $\pm x$ and $\pm y$ directions.

The limitation of this program is that the intersection of horizontal and vertical lines in a cross may not occur at a single pixel and thus, the program may not work at all. Also, its not necessary that the intensity value is always 255. Thus, we have to identify a range above which we may say that the color is black. Even this range might exclude the borderline values sometimes.

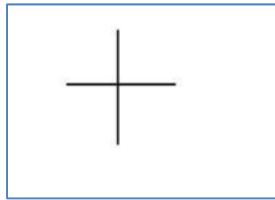


Figure 5.1 :circle and cross as targets

5.3 Circles as reference and target points and identifying circular objects: partially successful

Matlab image processing tools enable one to locate the boundaries of objects in an image. With the help of inbuilt functions, we can also estimate the area and perimeter of the objects. The value of the expression $4 \cdot \pi \cdot \text{area} / \text{perimeter}^2$ can be calculated for each object and the ones for which this value is close to 1 are circular. The centroids of these circular targets and references can be estimated from in-built functions. Thus, exact coordinates of a single point can be located. A single point gives more accurate results.

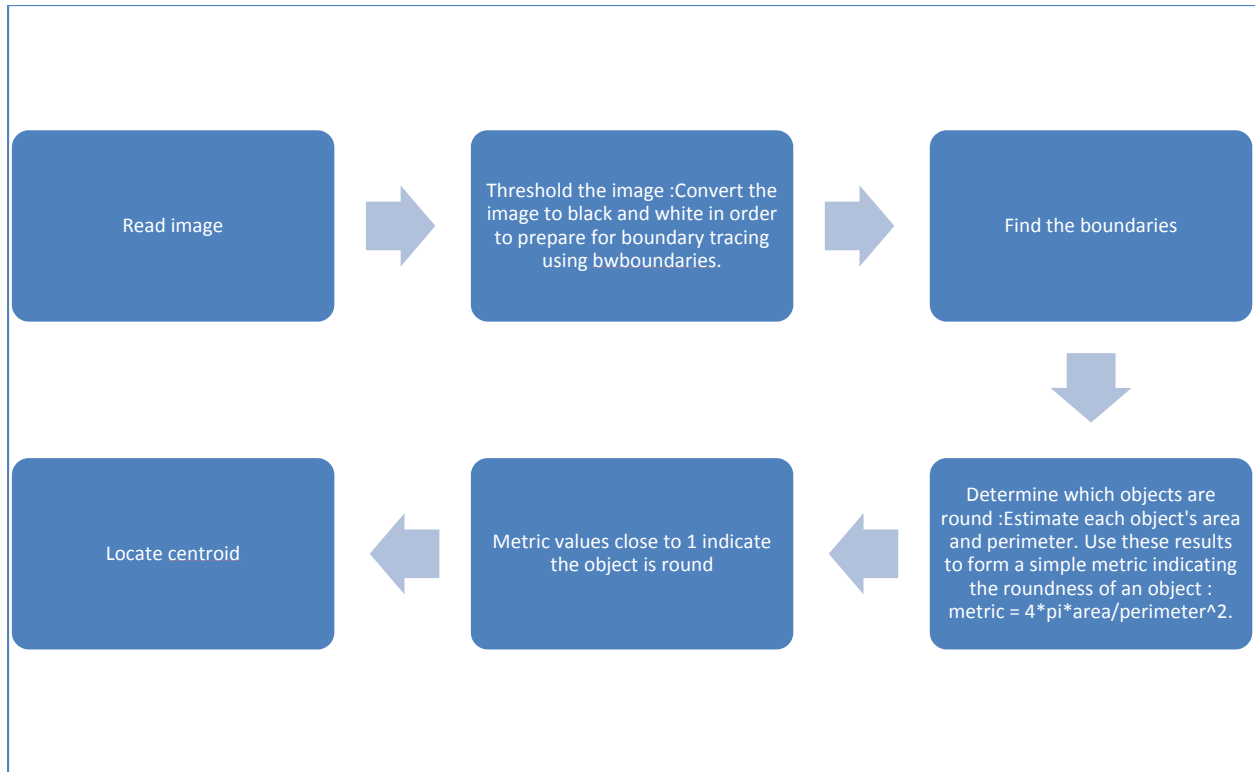


Fig. 5.2: Algorithm for attempt 3

Limitations:

1. An oblique view does not identify the object as a circle. Thus, a very low value of this threshold has to be chosen (as low as 0.6)
2. Many objects in the surroundings are identified as 'circular' with a low value of threshold. These points are unwanted and processing images with this program consumes a lot of space and time.

5.4 Circles as reference and target points and locating centroid after manual processing: successful

The unwanted objects are removed from the image, using paint and only the circular references and targets are exposed. The manually processed images are fed in the program that locates the boundaries of the objects and gives the centroid of each circle as the output. It does not identify circular objects and, in principle, any closed shape (circle, rectangle, triangle) can be used as

target. The coordinates are stored in the form of a matrix in MATLAB and the pixel values are used for calculating deflection.

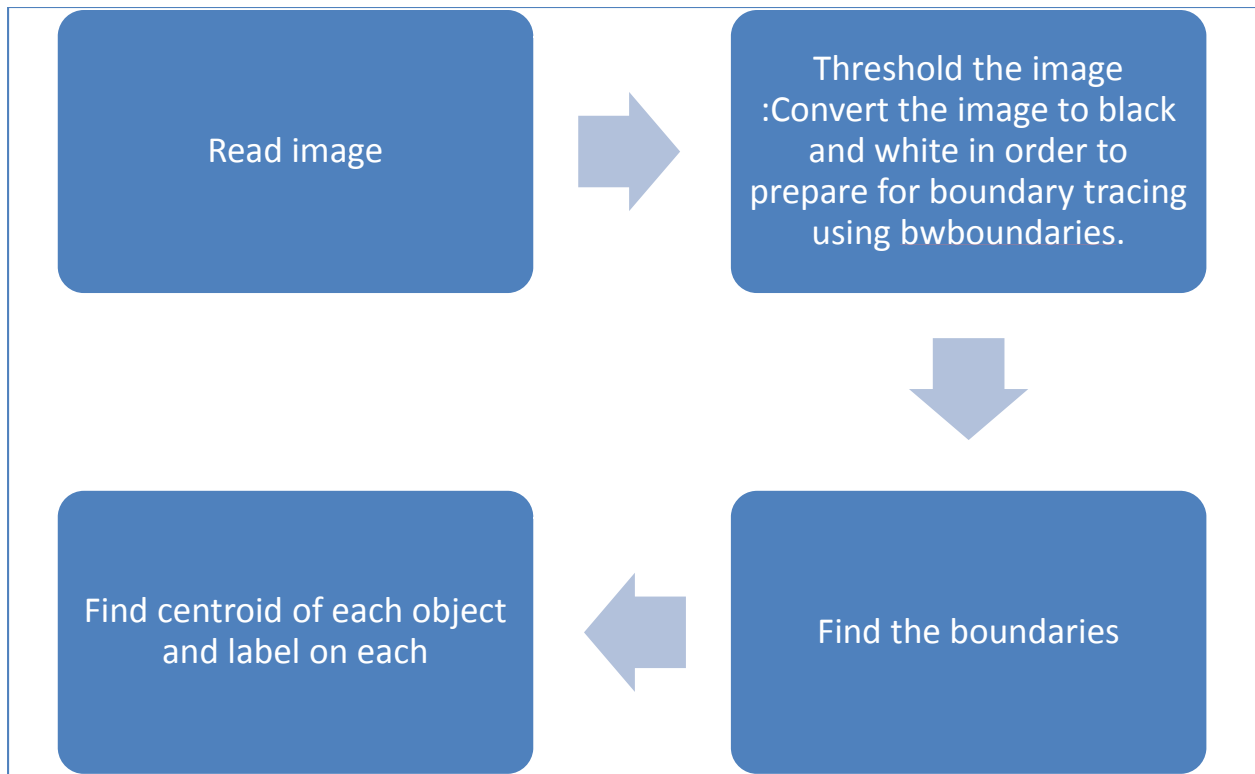


Fig. 5.3 Algorithm for attempt 4

CHAPTER 6

WORKING PROGRAM DETAILS

6.1 Image Processing

Image processing is the study of representation and manipulation of pictorial information. Digital image processing is performed on digital computers that manipulate images as arrays or matrices of numbers. The latest advancements in computer technology have opened the use of image processing analysis to fields that for their complexity would be impossible to be included in the past. High computational speed, high video resolution, more efficient computer language to process the data, and more efficient and reliable computer vision algorithms are some of the factors that let fields such as medical diagnosis, industrial quality control, robotic vision, astronomy, and intelligent vehicle / highway system to be included as a part of the large list of applications that use computer vision analysis to achieve their goals.

6.2 Grey-Level Segmentation/ Thresholding

Thresholding or grey-level segmentation is an essential concept related with image processing and machine vision. Thresholding is a **conversion between a grey-level image and a bilevel image**. Bilevel image is a monochrome image only composed by black and white pixels. It should contain the most essential information of the image (i.e., number, position and shape of objects), but is not comparable with the information offered by the grey-level image. Most of the time pixels with similar grey levels belong to the same object. Therefore, classifying the image by grey-level pixels may reduce and simplify some image processing operations such as pattern recognition, and classification.

The most essential thresholding operation will be the selection of a single threshold value. All the grey levels below this value are classified as black (0), and those above white (1). Most of time it is impossible to segment an image into objects and background with a single threshold value because of noise and illumination effects. A tentative simple approach could be the use of the mean grey level in the image as a threshold. This would cause about half of the pixels to become white and the other half black. (Martin, A. ; Tosunoglu,S., 2000)

6.3 Description of Program

The code for the required task was written using MATLAB, with the help of Image Processing Toolbox available with the language software. The following are the steps followed in the code:

1. **Read Image:** The image is read, pixel-by-pixel and stored in the form of a three-dimensional array.
2. **Threshold the image:** the image is converted to binary image (Black and White) in order to prepare it for boundary tracing.
3. **Find the boundaries:** the boundaries of all objects are traced and highlighted in bold. 'bwboundaries' returns a label matrix, labeling each object.
4. **Estimate each object's centroid:** the function 'regionprops' estimates the area and perimeter of each object. Stats(k).area returns the area and stats(k).centroid returns the coordinates of centroid of each object.
5. **Display the results:** the results are stored in the form of matrix and labeled on the image using the command (sprintf).

6.4 Final MATLAB Code

```
%% Identifying Round Objects
% To classify objects based on their roundness using
% [bwboundaries], a boundary tracing routine.
%
% Copyright 1993-2005 The MathWorks, Inc.
% $Revision: 1.1.6.3 $ $Date: 2005/12/12 23:21:52 $
%

%% Step 1: Read Image
% Read in |pills_etc.png|.

RGB = imread('22.jpg');
imshow(RGB);
```

```

%% Step 2: Threshold the Image
% Convert the image to black and white in order to prepare for
% boundary tracing using |bwboundaries|.

I = rgb2gray(RGB);
threshold = graythresh(I);
bw = im2bw(I,threshold);
imshow(bw)

%% Step 3: Find the Boundaries
% Concentrate only on the exterior boundaries. Option 'noholes' will
% accelerate the processing by preventing |bwboundaries| from searching
% for inner contours.

[B,L] = bwboundaries(bw);

% Display the label matrix and draw each boundary
imshow(label2rgb(L, @jet, [.5 .5 .5]))
hold on
for k = 1:length(B)
    boundary = B{k};
    plot(boundary(:,2), boundary(:,1), 'w', 'LineWidth', 2)
end

%% Step 5: Determine which Objects are Round
% Estimate each object's area and perimeter. Use these results
% to form a simple metric indicating the roundness of an object:
%
```

```

% metric = 4*pi*area/perimeter^2.
%
% This metric is equal to one only for a circle and it is less than one for
% any other shape. The discrimination process can be controlled by setting
% an appropriate threshold. In this example use a threshold of 0.94 so
% that only the pills will be classified as round.
%
% Use |regionprops| to obtain estimates of the area for all of the objects.
% Notice that the label matrix returned by |bwboundaries| can be
% reused by |regionprops|.

stats = regionprops(L,'Area','Centroid');

threshold = 0.85;
n = 0;

% loop over the boundaries
for k = 1:length(B)

    % obtain (X,Y) boundary coordinates corresponding to label 'k'
    boundary = B{k};

    % compute a simple estimate of the object's perimeter
    delta_sq = diff(boundary).^2;
    perimeter = sum(sqrt(sum(delta_sq,2)));

    % obtain the area calculation corresponding to label 'k'
    area = stats(k).Area;

    % compute the roundness metric
    metric = 4*pi*area/perimeter^2;

```

```

% display the results
metric_string = sprintf('object %d : %2.2f coordinates: %2.2f, %2.2f' , k, metric,
stats(k).Centroid);

% mark objects above the threshold with a black circle
%save coordinates of centroid for circular objects

if metric > threshold
    n = n+1;
    centroid = stats(k).Centroid;
    plot(centroid(1),centroid(2),'ko');
end

text(boundary(1,2)-35,boundary(1,1)+13,metric_string,'Color','y',...
'FontSize',14,'FontWeight','bold');

end

matrix = zeros (n,3);
i=1;

for k = 1: length(B)

    centroid = stats(k).Centroid;

```

```
matrix (i,1)=k;
matrix (i,2)= centroid(1);
matrix (i,3)= centroid(2);
i=i+1;

end

title(['Metrics closer to 1 indicate that ',...
      'the object is approximately round']);

displayEndOfDemoMessage(mfilename)
```

The output is in the form of coordinates of labeled objects. The coordinates of the reference and target points are now available. The distance between the reference and target points is calculated using the formulae from coordinate geometry. The difference in the value of these distances is the deflection.

6.5 Precision

Theoretically, precision of the method would depend on resolution of the camera and distance of camera from the image plane. If we assume that 1000 pixels measure 100 mm, each pixel would measure 0.1 mm. So, least count would depend on the camera resolution, image-camera distance and image processor. From the point of view of structural deformations, measurements of the order of 1 mm are sufficient. Thus, the precision of this method must be very high. But due to the limitations and sources of error discussed in chapter 8, this is usually not the case.

CHAPTER 7

APPLICATION ON WORKING EXPERIMENTS

The program was applied to different experimental setups in the structures laboratories to check its accuracy. A high resolution camera (7 Megapixel) was used. Targets and references were chosen as black colored circles. It was ensured that illumination is proper. Both the approaches 3 and 4 were applied. Approach 4 gave better results.

7.1 Schematic diagram

The first application was done on a schematic diagram drawn in “paint” application. The file is stored as a jpeg image. Fig. 7.1(a) is the unloaded beam and Fig. 7.1(b) is the loaded beam. The coordinates were labeled and the output files are shown in figs. 7.2(a) and 7.2(b). This is an **illustration** to the concept.

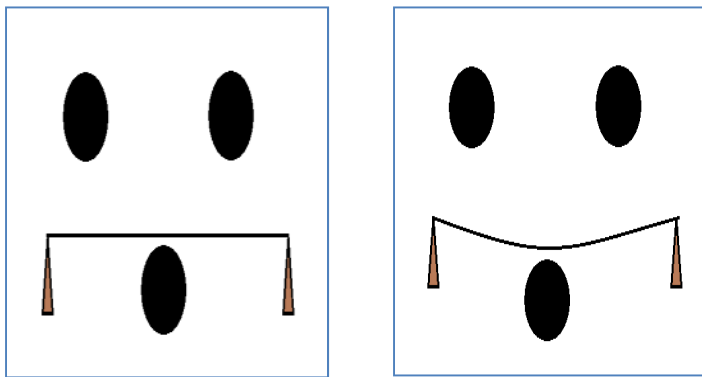


Fig. 7.1: Input files a. unloaded beam, b. loaded beam

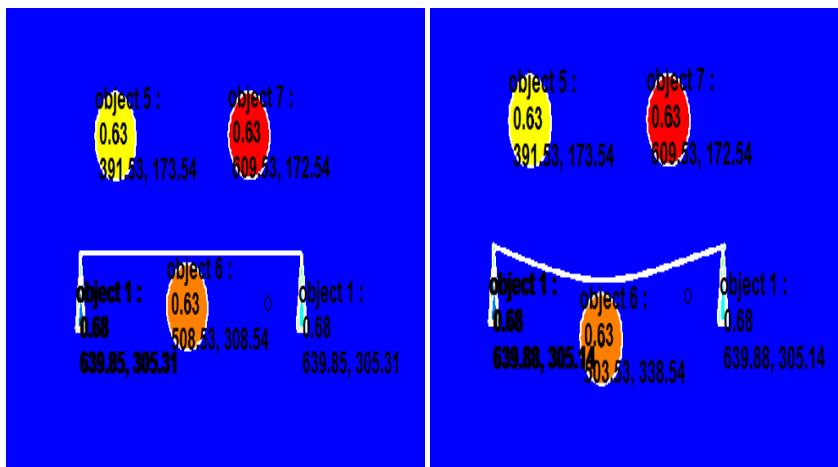


Fig. 7.2: output files a. unloaded beam, b. loaded beam

Distance between reference points (in pixels) = 218

Actual distance= 100mm (say)

Scaling factor= 100/218

Deflection= 30 pixels or $3000/218\text{mm} = 13.76 \text{ mm}$ (approx.)

7.2 Virtual lab setup (Smart Structural Dynamics Laboratory)

The SSDL lab has a setup for virtual labs where target and reference points are marked on a beam and its background. An off-the-shelf camera is mounted on a stand. The pictures were obtained from the official website of the laboratory at loaded and unloaded stages. Before feeding into the program, the images were manually processed in “paint” application to remove all unwanted objects.

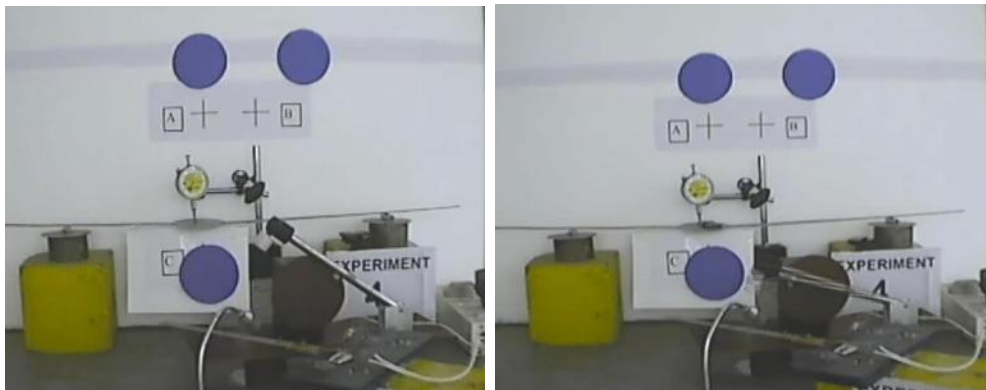


Fig. 7.3 initial pictures for a. unloaded beam, b. loaded beam

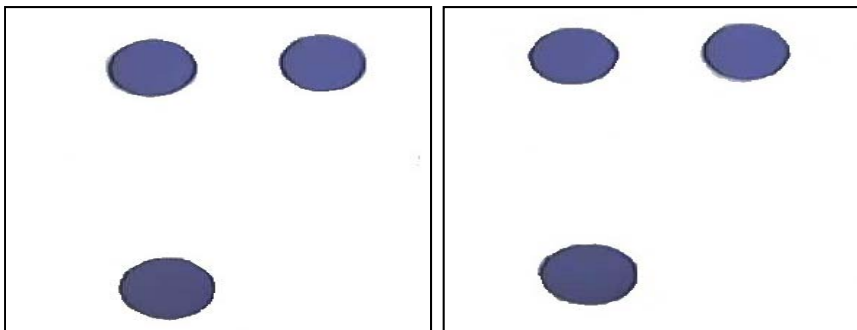


Fig. 7.4 Manually processed pictures for a. unloaded beam b. loaded beam

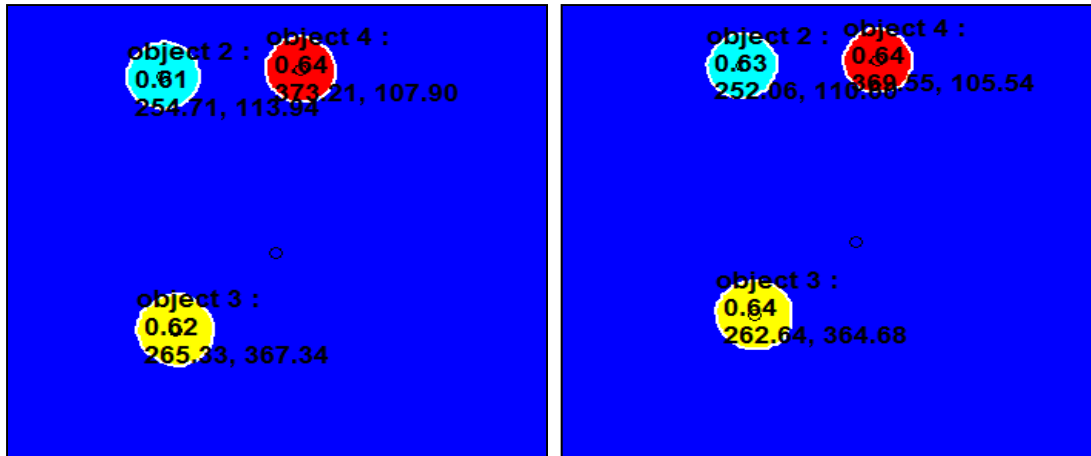


Fig. 7.5 :Output images for a. unloaded b. loaded beams

Table 7.1: calculations for virtual lab coordinates

	Reference 1		Reference 2		Target circle		Distance between references (pixels)	Distance between target and ref	Actual distance (mm)
	x	y	X	Y	x	Y			
Unloaded beam	254.71	113.94	373.21	107.90	265.33	367.34	118.65	259.44	437.73
Loaded beam	252.06	110.80	369.55	105.54	262.33	364.54	117.61	259	440.43

Displacement from photogrammetry= 2.71mm

Accounting for inclination of the camera, displacement= $2.71 / \cos 10 = 2.8\text{mm}$

Dial gauge reading= 3.75mm

The main reason for this difference in the two readings is that the reference and target points are not in the same plane. References are farther away from the target. Thus, scaling factor is lower than the actual value, hence, the displacement. There might be backlash error in the dial gauge also.

7.3 Concrete beam from the B.Tech Experiment

The concrete beam tested for load, deflection and strain for B.Tech course CEL232 (Reinforced Concrete Design) was fixed with a target point at its centre and two reference points at the front (fixed) table.



Fig. 7.6 sample picture for reinforced concrete beam photogrammetry experiment

The load versus displacement curves were obtained from the dial gauge readings as well as photogrammetry.

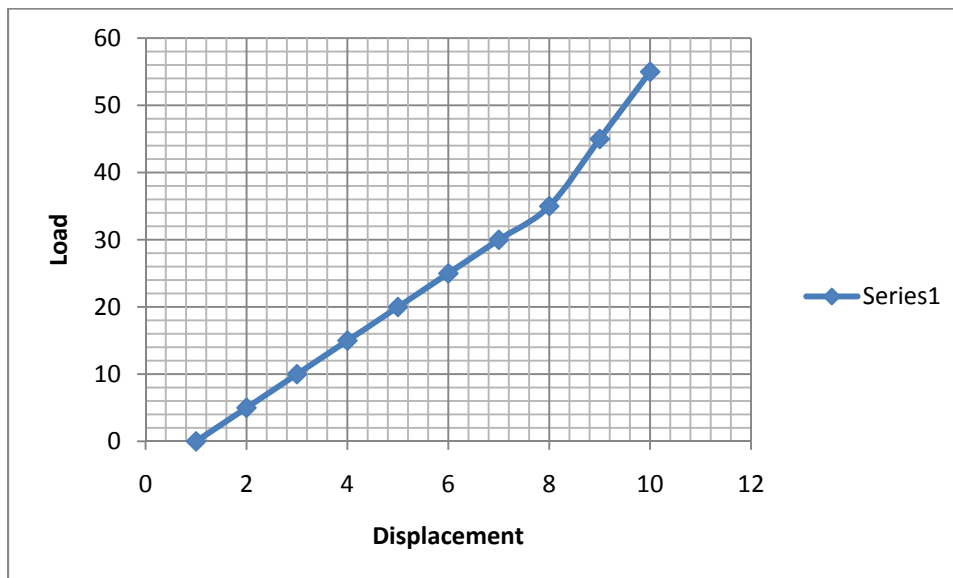


Fig. 7.7: Load versus deflection curve from dial gauge

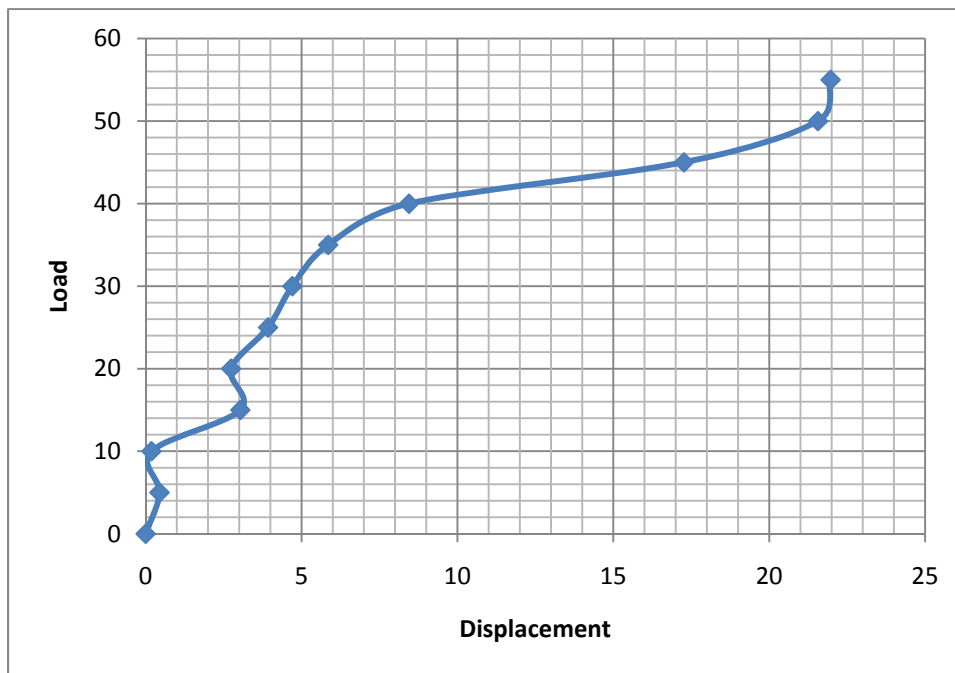


Fig. 7.8: Load versus deflection curve from photogrammetry

Although the trends followed are similar, but there is considerable difference in deflection values at failure. This may be attributed to the fact that references and target circle are not in the same plane and there may be an error due to calibration of dial gauge.

7.4 Structures Simulation Laboratory: Three experiments that are part of course CEL 331 Structural analysis 1) were analyzed using photogrammetry.

7.4.1 Measurement of tension in the arms by measuring deflection in the spring

Three springs with known value of force constants are provided. Loads can be put at two points. By knowing the displacement at springs, one can calculate the force in each of the three vertical links. The displacement values for the three joints were obtained by photogrammetry and compared with the actual displacement in the springs. The scale is drawn on the spring for measuring actual change in length.



Fig. 7.9: sample photograph for 7.4.1

The results are tabulated below:

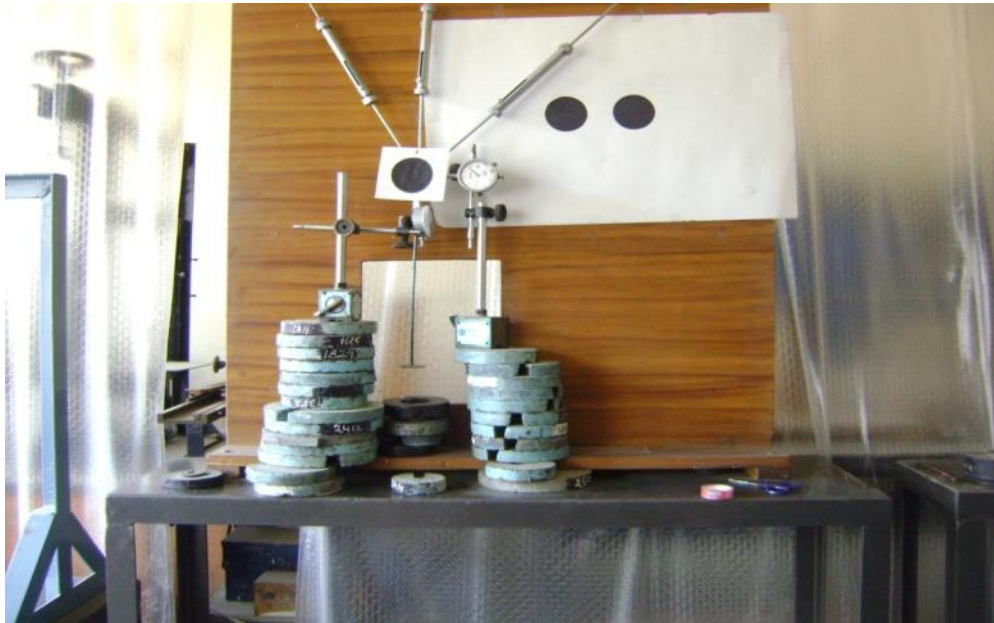
Table 7.2: calculations for 7.4.1

Trial number	Actual Displacement at spring 1	Displacement value from photogrammetry	Actual Displacement at spring 2	Displacement value from photogrammetry	Actual Displacement at spring 3	Displacement value from photogrammetry
1	2	2.9	1	2.3	3	1.9
2	5	5.1	5	5.4	4	4.2
3	3	3.2	7	7.5	10	9.3

7.4.2 **Horizontal and vertical deflection of point attached to multiple springs:** On putting different amounts of loads, the target circle moves by different amounts horizontally as well as vertically. This deflection is measured using dial gauge as well as photogrammetry. Calculations are given in **table 7.2**

Trial number	Horizontal Deflection (mm)		Vertical Deflection (mm)	
	Dial gauge	Photogrammetry	Dial gauge	Photogrammetry
1 (955g)	-0.98	-0.61	4.33	4.77
2 (448g)	-0.79	-0.71	0.42	1.29
3 (986g)	-1.8	-0.71	4.18	4.49

Fig. 7.10: sample picture for 7.4.2



The deflection values from dial gauge and from photogrammetry agree within acceptable deviations. Here, references and targets are in the same plane.

7.4.3 Two-point loading: The beam is loaded at two different points and dial gauges take deflection readings at the two points. The photogrammetric results are obtained by placing targets at required points. Since the magnitude of displacements is very low, percentage error is more.

Table 7.3: calculations for two-point loading

Trial number	Point 1		Point 2	
	Actual	Photogrammetry	Actual	photogrammetry
1	0.41	0.05	0.63	0.89
2	1.1	0.71	1.92	0.18
3	0.22	0.78	0.83	1.00

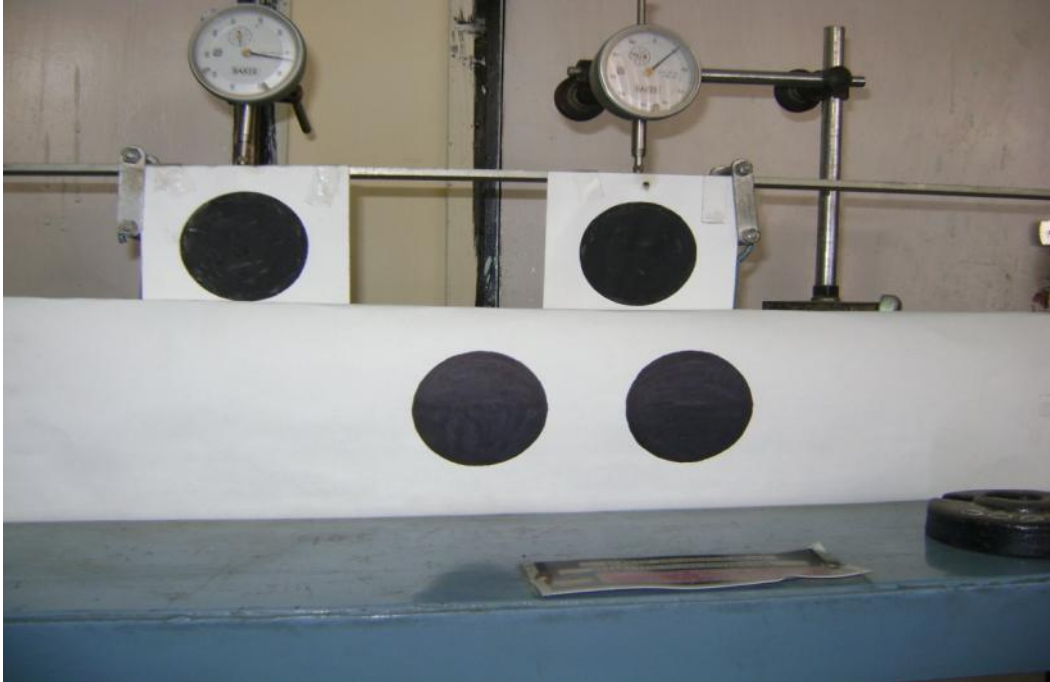


Fig. 7.11: Sample picture for 7.4.3

7.5 MTS Shake table- heavy structures lab

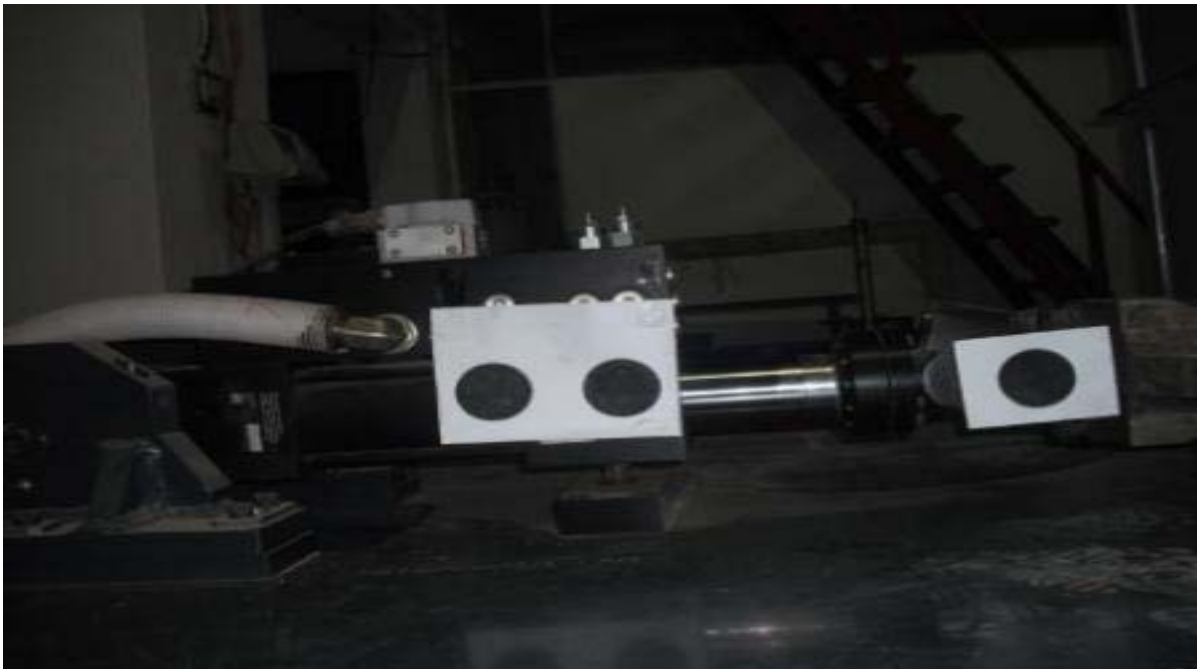


Fig. 7.12: Sample Picture for MTS Shake table

MTS shaketable can be given a displacement of desired value by connecting it to a computer and feeding the value. The displacement values are accurate and thus, it is a better check for the functioning of the program, since the actual displacement values are more reliable.

Table 7.4: calculations for MTS Shaketable

Values from photogrammetry	Actual values
1.05566	1
2.46969	2
3.92658	3
4.47351	4
4.83675	4.5
5.93414	5
5.43371	5.5
6.52703	6

Values from photogrammetry	Actual values
6.58318	6.5
6.11839	6
6.46203	5.5
5.57643	5
5.01424	4.5
3.53892	4
3.61747	3
2.30684	2
0.53881	1
0.54324	0

LIMITATIONS, PRECAUTIONS AND SOURCES OF ERROR

8.1 Limitations

- a. The above method can be used only for measuring planar deflections
- b. The reference and target points must be close.
- c. The deflected points must be visible and well-illuminated. For example, this method is inconvenient for measuring deflections under a slab, since a lot of illumination is required, along with different reference point pairs to account for different planes.
- d. The experimental apparatuses where the experiment is carried out must be free from vibration, since vibrations constantly alter the position of target point, giving a large error.
- e. Some initial manual processing is required before the digital processing.
- f. A high resolution camera increases the size of the image, thus making it difficult to process and a low resolution camera compromises on the accuracy of results.

8.2 Precautions

1. The reference and target points must be in the same plane

The principle of measurement is that the distance between the reference points is known and thus, the scale of the image, i.e., the pixel to distance conversion is known. This scale is applied to the If the reference and target points lie in the same plane, the conversion holds. The same number of pixels would measure a larger distance if a plane lies far off from the camera than if the plane were nearer.

2. The plane of the image must be parallel to plane containing references and targets

For the same reason as (1), the scale would change in this case too. Hence, the movement of the target must be confined to a single plane for measurement of this type. For three-dimensional movement, we need two cameras and principle of triangulation, which are out of the scope of this project.

3. The reference points and the camera must be perfectly horizontal

If not, we need extra calculations to account for movement at an angle to x and y axes.

4. The vibration disturbances to the apparatus must be minimized

The vibrations would keep changing the position of the targets and give wrong values.

5. The camera must lie approximately at the centroid of the three points to avoid oblique view

An oblique view would give a value that is lesser than the actual value of displacement. This is also a source of error, as, in many cases, it is not possible to eliminate oblique view.

6. All other objects must be eliminated from the image to avoid congestion

Removing unwanted objects would make the program faster and avoid congestion on the image viewer window.

CHAPTER 9

CONCLUSIONS

Photogrammetry technique has been applied to ongoing lab experiments and image processing program has been developed. The program gives accurate results for experiments involving readings in range of millimeters, but for very small values, results are not accurate. Also, static experiments free from vibrations give better results. Increasing the resolution of the camera and improving the capacity of the image processing machine gives better precision. Though having limitations, this method is cost-effective and accurate. It can be used for deflection measurements in virtual labs and thus, facilitate online experimentation. Also, it is of great importance when it comes to measurement of distances and deflections in inaccessible areas.

REFERENCES

1. Adams, L.P., (1975). "Henry Georges Fourcade", *Photogrammetric Record*, 8(45): 287-296.
2. Albota, M.G., (1976). "Short Chronological History of Photogrammetry", Proceedings of XIII Congress of the International Society for Photogrammetry, Commission VI, Helsinki, 20p.
3. Bales, F. B. (1985). "Close-range photogrammetry for bridge measurement." *Transportation Research Record 950*, Transportation Research Board, Washington, D.C., 39–44.
4. Bartel, J. (2001). "A picture of bridge health." *NTIAC (Nondestructive Testing Information Analysis Center) Newsletter*, 27(1), 1–4.
5. Fraser, C.S., (2000) Industrial measurement applications, in: *Close Range Photogrammetry and Machine Vision*, Whittles Publishing, Roseleigh House, Latheronwheel, Caithness, KW5 6DW, Scotland, UK , pp. 329–361.
6. *FotoG-FMS User Manual*. Vexcel Corporation, Boulder, Colo., 2000.
7. Forno, C., S. Brown, R. A. Hunt, A. M. Kearney, and S. Oldfield (1991) Measurement of Deformation of a Bridge by Moire Photography and Photogrammetry. *Strain*, Vol. 27, No. 3, pp. 83–87.
8. Hilton, M. H. (1985). "Application of close-range terrestrial photogrammetry to bridge structures." *Rep. VHTRC 85-R40*, Virginia Highway and Transportation Research Council, Charlottesville, Va.
9. Jauregui, V., White, K.R., Woodward, C.B., Leitch, K. (2003) "Noncontact Photogrammetric Measurement of Vertical Bridge Deflection" (ASCE)
10. Jauregui, V., White, K.R., Woodward, C.B., Leitch, K. (2007) Static Measurement of Beam Deformations via Close-Range Photogrammetry. *Transportation research record: journal of the transportation research board volume 1814/2002* pages 3-8.
11. **Martin, A; Tosunoglu,S.** (2000) "Image Processing Techniques for Machine Vision"
12. Mills, J., Barber, D (2004) Geomatics Techniques for Structural Surveying *Journal of Surveying Engineering*, - link.aip.org [Journal of Surveying Engineering 130, 56]

13. Nastasia, L. (1998) Digital Photo and Close-Range Photogrammetry Meet Surveying Tech for Highway Design and Maintenance. *Advanced Imaging*, Vol. 13, No. 1, pp. 46–48.
14. Scott, P. J. (1978) Structural Deformation Measurement of a Model Box Girder Bridge. *Photogrammetric Record*, Vol. 9, No. 51, pp. 361–378.
15. Woodhouse,N,G., Robson,S., Eyre,J.R., (1999) Vision metrology and three dimensional visualization in structural testing and monitoring, *Photogrammetric Record* 16 (94) 625–641.